

The Average Magnetic Field Strength in Molecular Clouds: New Evidence of Super–Alfvénic Turbulence

Paolo Padoan¹

*Department of Physics, University of California, San Diego, La Jolla, CA 92093-0424,
USA*

Raul Jimenez

*Department of Physics and Astronomy, University of Pennsylvania, Philadelphia, PA
19104, USA*

Mika Juvela

*Helsinki University Observatory, Tähtitorninmäki, P.O.Box 14, SF-00014 University of
Helsinki, Finland*

Åke Nordlund

*Copenhagen Astronomical Observatory and Theoretical Astrophysics Center, DK-2100,
Copenhagen, Denmark*

ABSTRACT

The magnetic field strength in molecular clouds is a fundamental quantity for theories of star formation. It is estimated by Zeeman splitting measurements in a few dense molecular cores, but its volume-averaged value within large molecular clouds (over several parsecs) is still uncertain. In this work we provide a new method to constrain the average magnetic field strength in molecular clouds. We compare the power spectrum of gas density of molecular clouds with that of two 350^3 numerical simulations of supersonic MHD turbulence. The numerical simulation with approximate equipartition of kinetic and magnetic energies (model A) yields the column density power spectrum $P(k) \propto k^{-2.25 \pm 0.01}$, the super–Alfvénic simulation (model B) $P(k) \propto k^{-2.71 \pm 0.01}$. The column density power spectrum of the Perseus, Taurus and Rosetta molecular cloud complexes is found to be well approximated by a power law, $P_o(k) \propto k^{-a}$, with $a = 2.74 \pm 0.07$, 2.74 ± 0.08 and 2.76 ± 0.08 respectively. We conclude that the observations are consistent with the presence of super–Alfvénic turbulence in molecular clouds (model B) while model A is inconsistent (more than 99% confidence) with the observations.

Subject headings: turbulence – ISM: kinematics and dynamics – radio astronomy: interstellar: lines

1. Introduction

The volume-averaged magnetic field strength in molecular clouds has never been measured directly. Zeeman splitting has been detected only from a few dense molecular cloud cores, where emission lines from molecules such as OH and CN are observed (Crutcher 1999; Bourke et al. 2001). Dense cores fill only a small fraction of the volume of molecular clouds. Therefore, the magnetic field strength averaged over the molecular cloud volume cannot be directly inferred from its value in the cores. This is true especially if the magnetic field strength has a very intermittent distribution and is correlated with the gas density, as suggested by Padoan & Nordlund (1999).

Estimates of magnetic field strength in molecular clouds have been inferred from the dispersion in the polarization angle (e.g. Myers & Goodman, 1991; Chrysostomou et al., 1994; Lai et al., 2001; Matthews & Wilson, 2002; Lai et al., 2002) as originally suggested by Davis (1951) and Chandrasekhar & Fermi (1953). This method was tested in numerical simulations of MHD turbulence by Ostriker et al. (2001), Padoan et al. (2001) and Heitsch et al. (2001). The relative motion of ions and neutral molecules, as manifested by a comparison of their spectral lines, has also been used to estimate the magnetic field strength in molecular clouds (Houde et al. 2000, 2002).

In this work we present a new way to constrain the average magnetic field strength in molecular clouds, based on the density power spectrum. In § 2 we show numerical simulations of supersonic MHD turbulence with different magnetic field strength yield different power spectra of gas density. The power spectrum is then computed from maps of molecular clouds in § 3. We find that only a rather low value for the average magnetic field strength, leading to super-Alfvénic turbulence, is consistent with the observations. Conclusions are summarized in § 4.

The density power spectrum depends on the rms sonic Mach number of the turbulence, M_S (the ratio of the rms flow velocity and the sound speed). In this work we use only simulations with $M_S \approx 10$ because that is the approximate value in the molecular cloud

¹padoan@jpl.nasa.gov

complexes we have studied. We do not study the dependence of the power spectrum on the value of M_S . In general, smaller values of M_S yield steeper density power spectra than the $M_S \approx 10$ models (this was verified with a set of simulations that will be presented elsewhere). Turbulent flows with $M_S \ll 1$, for example, are expected to generate a Kolmogorov density power spectrum, proportional to $k^{-11/3}$. This slope is comparable with the electron density power spectrum on very small scale estimated from scintillation studies (Armstrong et al. 1995). HI surveys of our galaxy and the Magellanic Clouds (Crovisier & Dickey 1983; Elmegreen et al. 2001; Stanimirović & Lazarian 2001; Dickey et al. 2001) produced power spectra with slope intermediate between the present results in molecular clouds and the scintillation studies.

2. Power Spectrum of Gas Density in Supersonic MHD Turbulence

In order to study the power spectrum of gas density, we have run two simulations of driven supersonic MHD turbulence with rms sonic Mach number $M_S \approx 10$ and isothermal equation of state. We have solved the three dimensional compressible MHD equations in a staggered mesh with 350^3 computational cells and periodic boundary conditions. The initial magnetic and density fields are uniform. The flow is driven by an external large scale random and solenoidal force, correlated at the largest scale turn-over time. The time derivative of the random force is generated in Fourier space, with power only in the range of wavenumbers $1 \leq k L_{\text{mesh}}/2\pi \leq 2$. The initial velocity field is proportional to the initial force, with an rms amplitude of approximately 50% of its relaxed value. Details about the numerical method are given in Padoan & Nordlund (1999).

We have run the simulations for five dynamical times. The dynamical time is here defined as $t_d = L_{\text{mesh}}/(2u)$, where u is the rms flow velocity. We choose this definition of dynamical time because the flow is forced up to wavenumber $k = 4\pi/L_{\text{mesh}}$ and therefore the largest turbulent scale is approximately $L_{\text{mesh}}/2$.

We characterize the simulations based on the relative importance of magnetic and dynamic (turbulent) pressure. The pressure ratio is defined as $P_m/P_d = \langle B^2 \rangle / [8\pi \langle \rho u^2 \rangle]$, averaging over the computational volume and over the last four dynamical times. In the first simulation (model A) the statistically relaxed pressure ratio is $P_m/P_d \approx 0.65 \pm 0.05$ (approximate equipartition of magnetic and kinetic energies). In the second simulation (model B), the ratio is $P_m/P_d \approx 0.09 \pm 0.01$ (kinetic energy of the turbulence approximately five times larger than magnetic energy). The standard deviation of approximately 10% in the pressure ratio of models A and B is due primarily to time fluctuations of the random force.

Power spectra have been computed for 18 times over the last four dynamical times (the small scale portions of these power spectra are statistically independent because the dynamical time decreases with spatial scale). The slopes are computed from a least square fit of the time-averaged power spectra plotted in Figure 4. We find that the power spectrum of the density field is sensitive to the pressure ratio (or the average magnetic field strength). The power spectrum of the three dimensional (3D) density field is $P(k) \propto k^{-2.25 \pm 0.01}$ in the equipartition run (model A) and $P(k) \propto k^{-2.70 \pm 0.01}$ in the super-Alfvénic case (model B).

In isotropic turbulence the power spectrum of the projected density is the same as the power spectrum of the 3D density field (not necessarily in the presence of a mean magnetic field or in real molecular clouds). We have verified this in our numerical data. We have also verified that the power spectrum of the projected density does not depend on the direction of projection relative to the direction of the mean magnetic field. However, our results are based on the power spectra of the 3D density field and not of the projected density, because the statistical sample size is reduced by the projection (larger noise in 2D power spectra than in 3D ones).

3. Power Spectrum of Column Density in Molecular Clouds

The distribution of column density in molecular clouds can be estimated from maps of the J=1-0 ^{13}CO emission line. In this work we use J=1-0 ^{13}CO maps of the Perseus (Padoan et al. 1999), Taurus (Mizuno et al. 1995) and Rosetta (Heyer & et al. 2003) molecular cloud complexes and find the power spectrum of projected density in these regions is well approximated by a power law, $P_o(k) \propto k^{-a_o}$.

The value of the gas column density inferred from the J=1-0 ^{13}CO maps depends on the distribution of ^{13}CO abundance and J=1-0 ^{13}CO excitation temperature, T_{ex} . The column density can be estimated using the LTE method (Dickman 1978; Harjunpää & Mattila 1996; Padoan et al. 1998a). In the LTE method the value of T_{ex} along each line of sight is assumed to be constant and is estimated using the observed peak temperature, $T_r = T_p$, of an optically thick line ($\tau \gg 1$) in the equation:

$$T_r = [J(T_{\text{ex}}) - J(T_{\text{bg}})](1 - e^{-\tau}) \quad (1)$$

where $T_{\text{bg}} = 2.7$ K is the background temperature, and the function $J(T)$ is defined as:

$$J(T) = \frac{T_0}{\exp(T_0/T) - 1} \quad (2)$$

with $T_0 = h\nu_{10}/k$ and ν_{10} is the frequency of the J=1-0 ^{13}CO transition. The J=1-0 ^{12}CO transition, when available, is generally used as the optically thick line to estimate the value

of T_{ex} . For the present analysis we apply the LTE method using only the J=1-0 ^{13}CO line because ^{12}CO maps are not available to us. This line is optically thick only in the brightest regions of the maps used in the present work. The value of T_{ex} can be estimated from the J=1-0 ^{13}CO line only in those regions. Therefore, we use the peak temperature of this line over the whole map to estimate the value of T_{ex} as outlined above. This single value of T_{ex} is used for all map positions (the effect of this assumption is addressed below with radiative transfer calculations). Finally, the ^{13}CO column density is given by:

$$N_{\text{LTE}} = 6.39 \times 10^{14} Q \frac{\sum_v \tau(v) \Delta v}{1 - e^{-T_0/T_{\text{ex}}}} \quad (3)$$

where $\tau(v)$ is the optical depth in the velocity channel corresponding to the velocity v and is estimated from equation (1) using the estimated value of T_{ex} and the radiation temperature $T_{\text{r}}(v)$ given by the observed line profile. Δv is the width of the velocity channels in the observations, expressed in km/s, and the partition function Q is assumed to be a constant over the map so its value is not required as it does not affect the slope of the density power spectrum.

Column density maps of the Perseus, Taurus and Rosetta regions have been computed from the observed J=1-0 ^{13}CO spectral maps with this simplified LTE method. Their power spectra are plotted in Figure 4. They are shown to be well approximated by power laws over one decade or more in wavenumber, $P_o(k) \propto k^{-a_o}$, with $a_o \approx 2.87 \pm 0.04$ for Perseus, $a_o \approx 2.87 \pm 0.06$ for Taurus and $a_o \approx 2.89 \pm 0.06$ for Rosetta.

In order to estimate the effect of assuming constant Q and T_{ex} , the simplified LTE method for estimating the gas column density has been applied to synthetic spectra. Assuming a uniform ^{13}CO abundance, synthetic spectral maps of the J=1-0 ^{13}CO line have been computed with a 3D non-LTE Monte Carlo radiative transfer code (Juvola 1997) as described in Padoan et al. (1998b). The radiative transfer is computed through the density and velocity field of two snapshots of model B (at 3 and 4 dynamical times), regridded to a resolution of 175^3 , assuming average density $\langle n \rangle = 500 \text{ cm}^{-3}$ and mesh size $L_{\text{mesh}} = 10 \text{ pc}$. The 3D distribution of kinetic temperature is computed self-consistently as part of the radiative transfer solution, from the balance of cosmic ray heating and molecular and atomic cooling. We have assumed a cosmic ray hydrogen ionization rate of $2 \times 10^{-17} \text{ s}^{-1}$ and heating of 8 eV per ionization.

Six maps of 175×175 synthetic J=1-0 ^{13}CO lines are obtained in this way, corresponding to three orthogonal directions of projection of the two 3D snapshots. The simplified LTE method is then applied to these six synthetic spectral maps and the estimated column density is compared with the actual column density in the original snapshots of model B. The result for one of the maps is plotted in Figure 4. Figure 4 shows the estimated column density,

N_{LTE} , is roughly proportional to the true column density, but tends to saturate at large column density values. This is due both to the low gas temperature and to the J=1-0 ^{13}CO line saturation in the densest regions. The power spectra of the column density field estimated from the synthetic spectral map, $P_{\text{LTE}}(k) \propto k^{-a_{\text{LTE}}}$, are then compared with the power spectra computed directly from the projections of the original MHD data cube, $P_{\text{MHD}}(k) \propto k^{-a_{\text{MHD}}}$.

We find that $P_{\text{LTE}}(k)$ is generally steeper than $P_{\text{MHD}}(k)$. This is primarily due to the decreased emission from the densest regions due to their low gas temperature and to the saturation of the J=1-0 ^{13}CO line. The difference is $a_{\text{LTE}} - a_{\text{MHD}} = 0.13 \pm 0.06$. If this correction is applied to the observed molecular cloud complexes, the corrected power spectrum has a slope $a = 2.74 \pm 0.07$ for Perseus, $a = 2.74 \pm 0.08$ for Taurus and $a = 2.76 \pm 0.08$ for . At the 1σ level, model B is consistent with these molecular cloud complex power spectra, while the power spectrum of model A is inconsistent with the observations with virtually 100% confidence (7σ).

Variations in ^{13}CO abundance may affect the estimated column density. However, significant CO depletion is expected only above 10 magnitudes of visual extinction and the CO abundance should drop only below 1-2 magnitudes. Most of the gas mass in molecular cloud complexes emits at values of visual extinction between 1 and 10 mag. Therefore, the effect of gas temperature variations estimated above should be more important than the neglected effect of variations in ^{13}CO abundance.

4. Conclusions

The average magnetic field strength in molecular clouds cannot be measured directly. However, it can be inferred from observational data due to its effect on the gas dynamics. In this work we have found the power spectrum of the density field is a sensitive diagnostic of the magnetic field strength. Numerical simulations of supersonic MHD turbulence with rms sonic Mach number $M_S \approx 10$ develop a power law power spectrum of gas density, $P_{\text{MHD}}(k) \propto k^{-a_{\text{MHD}}}$. The value of the power law exponent is $a_{\text{MHD}} = 2.25 \pm 0.01$ when the flow rms velocity is comparable to the Alfvén velocity and $a_{\text{MHD}} = 2.71 \pm 0.01$ in the super-Alfvénic simulation.

The density power spectrum can be measured also in molecular cloud complexes, for example using J=1-0 ^{13}CO maps. However, the column density (and its power spectrum) estimated using only the J=1-0 ^{13}CO line and the LTE method are biased by a number of uncertainties. The most significant uncertainties are the 3D distribution of the gas kinetic

temperature in the molecular cloud complexes and the saturation of the J=1-0 ^{13}CO line in very dense regions. We have investigated the effect of these uncertainties in the density power spectrum using synthetic J=1-0 ^{13}CO spectral maps computed with a non-LTE Monte Carlo radiative transfer code. The 3D equilibrium temperature distribution is computed self-consistently as part of the radiative transfer solution by balancing cosmic ray heating with molecular and atomic cooling. The correct power spectrum slope, a_{MHD} , is found to be smaller than the slope estimated with the LTE method, a_{LTE} , with $a_{\text{MHD}} = a_{\text{LTE}} - 0.13 \pm 0.06$.

With this correction, the power spectrum slope is $a = 2.74 \pm 0.07$ for Perseus, $a = 2.74 \pm 0.08$ for Taurus and $a = 2.76 \pm 0.08$ for Rosetta. The super-Alfvénic model is consistent with this result, while the model with rms flow velocity comparable to the Alfvén velocity is ruled out by the observations. This is yet another indication that super-Alfvénic turbulence provides a good description of molecular cloud dynamics. As first proposed by Padoan & Nordlund (1997, 1999), the average magnetic field strength in molecular clouds may be much smaller than required to support them against the gravitational collapse. Evidence of super-Alfvénic turbulence was also found recently by Troland and Heiles (2001) in HI clouds.

MJ acknowledges the support from the Academy of Finland Grants no. 174854 and 175068. Computing time was provided by the Danish Center for Scientific Computing. The research of RJ is partially supported by NSF grant AST-0206031.

REFERENCES

- Armstrong, J. W., Rickett, B. J., & Spangler, S. R. 1995, *ApJ*, 443, 209
- Bourke, T., Myers, P., Robinson, G., & Hyland, H. 2001, *ApJ*
- Chandrasekhar, S. & Fermi, E. 1953, *ApJ*, 118, 113
- Chrysostomou, A., Hough, J. H., Burton, M. G., & Tamura, M. 1994, *MNRAS*, 268, 325
- Crovisier, J. & Dickey, J. M. 1983, *A&A*, 122, 282
- Crutcher, R. M. 1999, *ApJ*, 520, 706
- Davis, L. 1951, *Physical Review*, 81, 890
- Dickey, J. M., McClure-Griffiths, N. M., Stanimirović, S., Gaensler, B. M., & Green, A. J. 2001, *ApJ*, 561, 264

- Dickman, R. L. 1978, *ApJS*, 37, 407
- Elmegreen, B. G., Kim, S., & Staveley-Smith, L. 2001, *ApJ*, 548, 749
- Harjunpää, P. & Mattila, K. 1996, *A&A*, 305, 920
- Heitsch, F., Zweibel, E. G., Mac Low, M., Li, P., & Norman, M. L. 2001, *ApJ*, 561, 800
- Heyer, M. H. & et al. 2003, in preparation
- Houde, M., Bastien, P., Dotson, J. L., Dowell, C. D., Hildebrand, R. H., Peng, R., Phillips, T. G., Vaillancourt, J. E., & Yoshida, H. 2002, *ApJ*, 569, 803
- Houde, M., Bastien, P., Peng, R., Phillips, T. G., & Yoshida, H. 2000, *ApJ*, 536, 857
- Juvela, M. 1997, *A&A*, 322, 943
- Lai, S., Crutcher, R. M., Girart, J. M., & Rao, R. 2001, *ApJ*, 561, 864
- . 2002, *ApJ*, 566, 925
- Matthews, B. C. & Wilson, C. D. 2002, *ApJ*, 574, 822
- Mizuno, A., Onishi, T., Yonekura, Y., Nagahama, T., Ogawa, H., & Fukui, Y. 1995, *ApJL*, 445, L161
- Myers, P. C. & Goodman, A. A. 1991, *ApJ*, 373, 509
- Ostriker, E. C., Stone, J. M., & Gammie, C. F. 2001, *ApJ*, 546, 980
- Padoan, P., Bally, J., Billawala, Y., Juvela, M., & Nordlund, Å. 1999, *ApJ*, 525, 318
- Padoan, P., Goodman, A., Draine, B. T., Juvela, M., Nordlund, Å., & Rögnvaldsson, Ö. E. 2001, *ApJ*, 559, 1005
- Padoan, P., Juvela, M., Bally, J., & Nordlund, Å. 1998a, *ApJ*, in press
- . 1998b, *ApJ*, 504, 300
- Padoan, P. & Nordlund, Å. 1997, *astro-ph/9706176*
- . 1999, *ApJ*, 526, 279
- Stanimirović, S. & Lazarian, A. 2001, *ApJL*, 551, L53
- Troland, T. H. & Heiles, C. 2001, American Astronomical Society Meeting, 198, 0

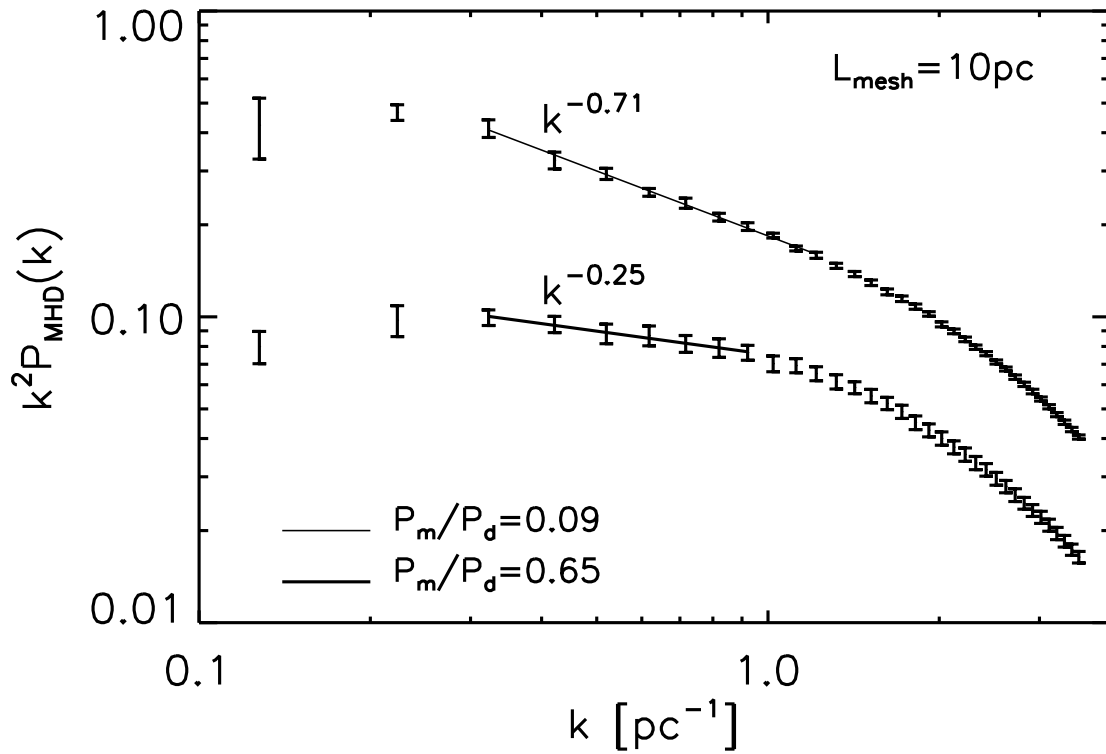


Fig. 1.— Time-averaged density power spectra of model B (upper plot), and model A (lower plot). The solid lines are least square fits in the range $0.3\text{--}0.9 \text{ pc}^{-1}$ for model A and $0.3\text{--}1.2 \text{ pc}^{-1}$ for model B, assuming a mesh size $L_{\text{mesh}} = 10 \text{ pc}$.

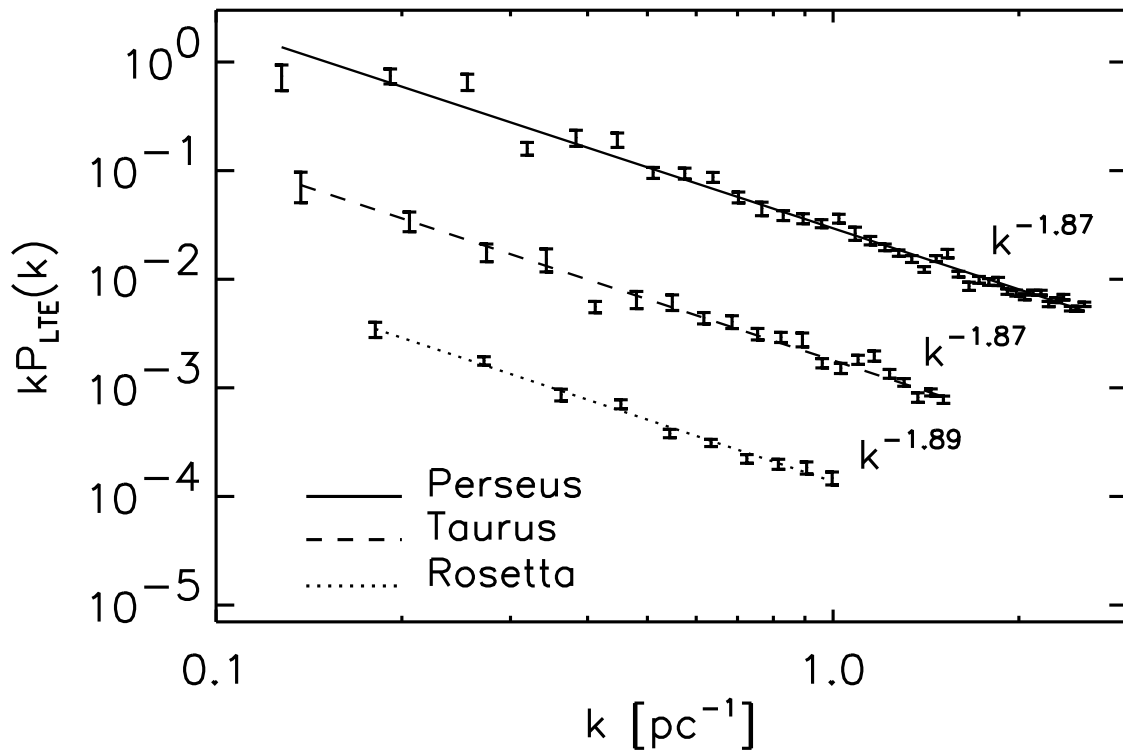


Fig. 2.— Power spectra of three molecular cloud complexes. The power spectra are computed from images of column density obtained with the LTE method applied to maps of the J=1-0 ^{13}CO emission line.

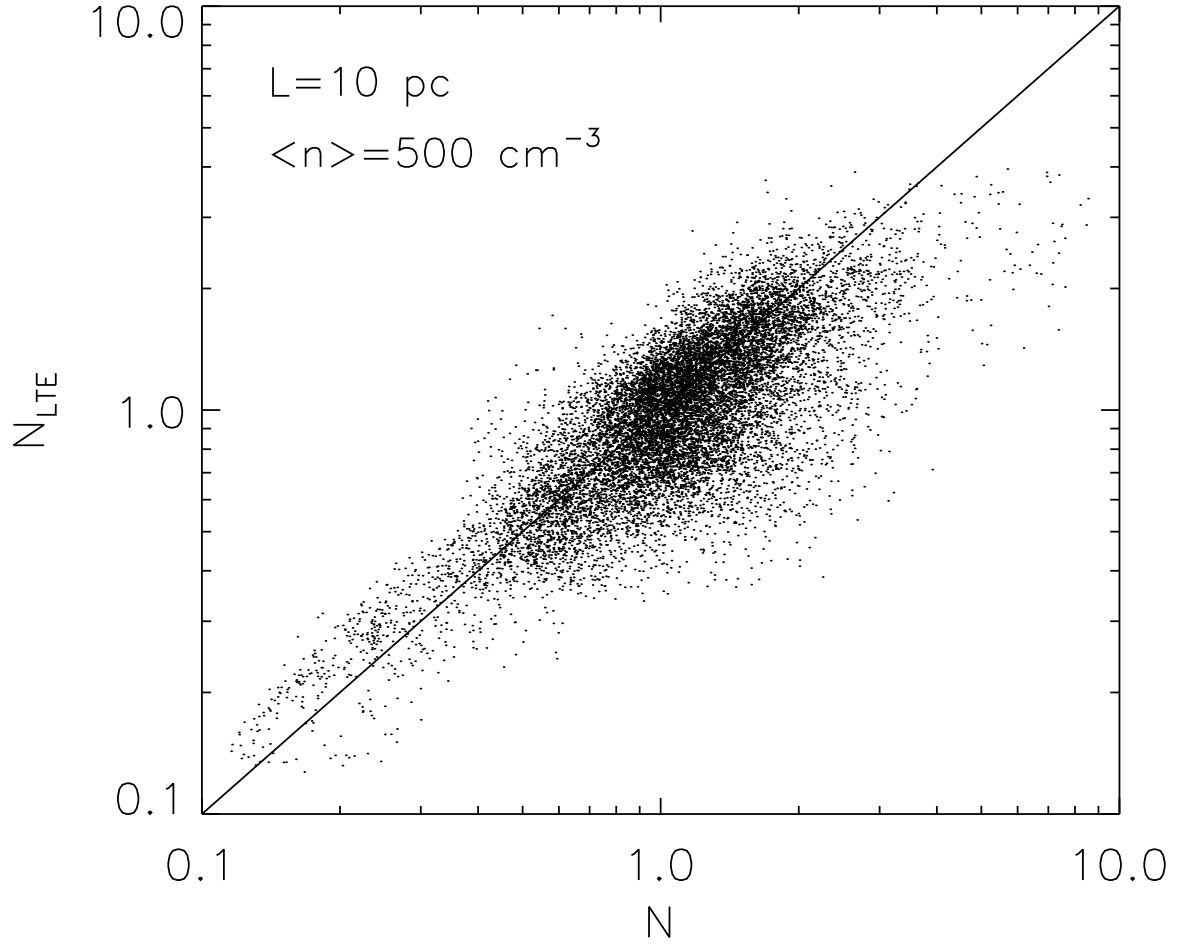


Fig. 3.— Scatter plot of column density estimated with the LTE method applied to a synthetic map of the $J=1-0$ ^{13}CO emission line versus the column density in the MHD data cube used to compute the synthetic spectra.